Simulation of a tractor-implement model under the influence of lateral disturbances

Author:
Pota, Himanshu; Katupitiya, Jayantha; Eaton, Ray

Publication details:
Proceedings of the IEEE International Conference on Decision and Control
pp. 596-601

Event details:
IEEE Conference on Decision and Control
New Orleans, USA

Publication Date:
2007

Publisher DOI:
http://dx.doi.org/10.1109/CDC.2007.4434953

Simulation of a tractor-implement model under the influence of lateral disturbances

Hemanshu Pota, Jayantha Katupitiya, and Ray Eaton

***Abstract*— This work presents the derivation of a comprehensive mathematical model for an off-road vehicle such as an agricultural tractor that drags behind it a heavy implement. The models are being developed with the aim of designing robust controllers that will enable the high precision control of the implement's trajectory. The developed model is subjected to real conditions, such as ground undulation and uncertainty, sloping terrain, tyre slippage, and constrained steering of the tractor. The implement is assumed to possess independently steered wheels for aiding in implement alignment. A complete model is presented and simulated under varying conditions. Primarily this work demonstrates and validates the trailed vehicle system behavior when the trailing implement is subjected to large drag forces due to ground engagement and the significantly large lateral disturbances that occur in real life broad acre farming conditions.**

I. INTRODUCTION

Precision farming is aimed at ensuring spatial precision of on-farm agricultural tasks. The reducing labour availability, increasing labour costs and the emergence of corporate style farming has placed a new emphasis on precision farming with the possibility of fully autonomous farming in the future. The aim is to minimise the degree of complexity of mechanical manipulation so that large scale machinery can be used with cost effectiveness and reliability. It is a well known fact that, the more structured the environment is, the easier it is to apply robotic solutions. Given the large scale nature of agricultural operations, a structured farming system is extremely desirable.

Structured farming commences at the layout stage of the farming system. During layout, the traffic directions can be chosen to minimise undesirable effects of gravitational forces, maximise straight runs, avoid mixing up different soil conditions and so forth. In existing farms, the precision farming effort is largely directed at the seeding stage. If the crop can be planted at desired locations as determined by a precision farming data set that ensures optimised machinery performance, all follow up operations such as weeding and fertilising becomes simpler and hence easier to automate.

As of today, precision tractor guidance is well established. Within limited disturbances the tractors can ensure sub-inch precision. Given this ability, controlled traffic has been introduced, in which the tractor wheels are expected to travel within pre-specified tracks. Tractors traveling outside these tracks are considered undesirable and cause damage to the soil structure. Unfortunately, the actual agricultural tasks are carried out by the implements and not by the tractors. The precision guidance of the tractor does not directly translate into the precision guidance of the implement. Unlike the tractors, the implements, especially the seeding implements, are subject to significant ground contact forces and hence there is a large set of disturbance forces that cause the implements to drift off course. Among these disturbances are; the uneven ground contact forces due to varying soil structure across the width of the implement, gravitational forces on sloping land and the effects of lateral undulations that may cause some of the seeding tines to dig deeper than the others thereby generating unbalanced forces.

Almost all research in the area of mobile platforms has been done for non-holonomic constrained (assuming no side-slip) systems [1], [2]. This assumption is valid for most mobile platforms. Most results, for this class of systems, are available through purely velocity kinematic models [1]. However, the off-axle hitched implement and tractor system does not satisfy the standard assumptions needed to solve the non-holonomic constrained velocity kinematics thus special methods are developed for it [3]. This makes the control problem with full-dynamics (mass, inertia, etc.) even more difficult. In the literature, modeling of agricultural vehicles has been presented [4] and their precision guidance has been achieved to a great extent [5], [6], [7]. A three-point mounted implement guidance system has also been tested for its performance [8], [9]. However, these systems only guarantee accurate motion of the prime mover. They do not present a control methodology for precision guidance of the implements subject to significant disturbance forces while taking into account the actual tractor-implement dynamics.

In this paper, we present a complete mathematical model that takes in to account the dynamics of a tractor and an implement. The paper presents two models; the non-slip model that represents the ideal performance and the slip model that represents what may be encountered in practice. The tractor is modeled as a front wheel steered machine with either four wheel propulsion or rear wheel propulsion. It has an off axle hitch point to which the trailing implement is attached. The implement is subjected to a significant drag force due to ground contact. The trailing wheels of the implement can be steered.

H. Pota is with the School of Information Technology and Electrical Engineering, The University of New South Wales @ Australian Defence Force Academy, h.pota.unsw.edu.au

J. Katupitiya is with the School of Mechanical and Manufacturing Engineering, The University of New South Wales, j.katupitiya@unsw.edu.au

R. Eaton is with the School of Electrical Engineering and Telecommunications, The University of New South Wales, r.eaton@unsw.edu.au

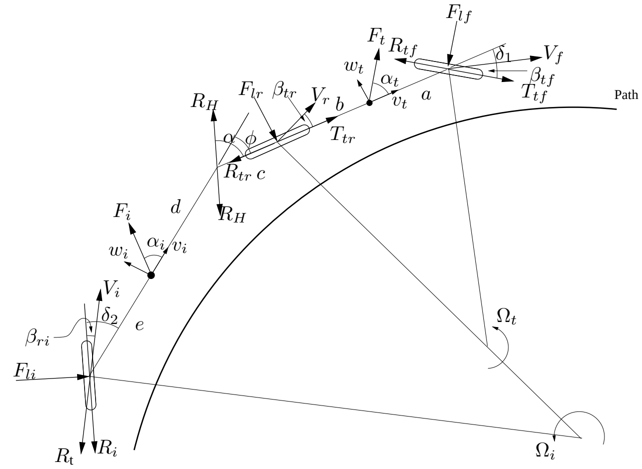

Fig. 1. Tractor Implement set up in a slipping condition subjected to disturbance forces of F_t and F_i

II. DYNAMIC MODEL DEVELOPMENT

Fig. 1 shows an off-axle coupled steerable implement being pulled by a tractor. For simplicity, all pairs of wheels are represented by single wheels along the longitudinal axis of the tractor and the implement. Note that this represents a lateral slip situation with β_{tf}, β_{tr} and β_{ri} being the three slip angles of the tractor's front wheels, tractor's rear wheels and the implement wheels, respectively. Tractor has two propulsion forces T_{tf} and T_{tr} at the front wheels and rear wheels, respectively. Tractor's steering angle is δ_1 and the implement's steering angle is δ_2. All three wheels are subjected to the three rolling resistances R_{tf}, R_{tr} and R_i as shown in Fig. 1. In addition to these, the implement is subjected to the implement drag force of R_t acting in the direction directly opposite to the direction of travel of the implement. The tractor's velocities at its centre of mass are v_t in the longitudinal direction and w_t in the lateral direction. Similarly, the velocities of the implement at its centre of mass are, v_i and w_i. The inertias of the tractor and the implement, at their centre's of mass are I_t and I_i, respectively. The tractor mass is m_t and that of the implement is m_i. The angular velocities of the tractor and the implement are Ω_t and Ω_i. R_H is the hitch point reaction and ϕ is the tractor-implement misalignment.

By equating the velocities at the hitch point, the following two equations can be written.

$$\begin{aligned} v_t &= v_i \cos\phi - (w_i + d\Omega_i)\sin\phi && (1) \\ w_t &= (w_i + d\Omega_i)\cos\phi + v_i \sin\phi + (b+c)\Omega_t && (2) \end{aligned}$$

A. Slip Model

Six dynamic equations can be written with three for the tractor (two translational and one rotational) and three for the implement. Equations (1) and (2) can be used to eliminate v_t and w_t to obtain four equations in the four state variables $\{v_i, w_i, \Omega_t, \Omega_i\}$. These can then be expressed as,

$$D \begin{bmatrix} \dot{v}_i \\ \dot{w}_i \\ \dot{\Omega}_t \\ \dot{\Omega}_i \end{bmatrix} + G_{1_1} \begin{bmatrix} F_{lf} \\ F_{lr} \\ F_{li} \end{bmatrix} + G_{1_2} \begin{bmatrix} R_{tf} \\ R_{tr} \\ R_i \\ R_t \end{bmatrix} + G_2 \begin{bmatrix} T_{tf} \\ T_{tr} \end{bmatrix} + G_3 \begin{bmatrix} F_i \\ F_t \end{bmatrix} + G_0 = 0 \quad (3)$$

Equation (3) represents the simulation model. The dynamic model given below is obtained by ignoring disturbance forces.

$$D \begin{bmatrix} \dot{v}_i \\ \dot{w}_i \\ \dot{\Omega}_t \\ \dot{\Omega}_i \end{bmatrix} + G_{1_1} \begin{bmatrix} F_{lf} \\ F_{lr} \\ F_{li} \end{bmatrix} + G_2 \begin{bmatrix} T_{tf} \\ T_{tr} \end{bmatrix} + G_0 = 0 \quad (4)$$

See Appendix for the D matrix and the G matrices of (3). A complete set of dynamic equations can be obtained by appending the following three equations.

$$\begin{aligned} \dot{\phi} &= \Omega_i - \Omega_t && (5) \\ \dot{\delta}_1 &= F_{st} && (6) \\ \dot{\delta}_2 &= F_{si} && (7) \end{aligned}$$

where F_{st} and F_{si} are the steering inputs of the tractor and the implement, respectively. Equations (4), (5)-(7) form the complete set of dynamic equations for the slip model with the state vector of $\{v_i, w_i, \Omega_t, \Omega_i, \phi, \delta_1, \delta_2\}^T$ and a control input vector of $\{T_{tf}, T_{tr}, F_{st}, F_{si}\}^T$. The position and orientation of the implement can be obtained by integrating the following equations.

$$\begin{aligned} \dot{\theta}_i &= \Omega_i && (8) \\ \dot{x}_i &= v_i \cos\theta_i - w_i \sin\theta_i && (9) \\ \dot{y}_i &= v_i \sin\theta_i + w_i \cos\theta_i && (10) \end{aligned}$$

For the purpose of simulation, each rolling resistance has two terms, a viscous type term that is proportional to the rolling velocity and another term that is proportional to the normal load on each wheel.

To determine the slip forces, the slip angles must be calculated. The lateral slip angles are,

$$\begin{aligned} \beta_{ft} &= \tan^{-1}\frac{(w_t + a\Omega_t)}{v_t} + \delta_1 && (11) \\ \beta_{rt} &= \tan^{-1}\frac{(w_t - b\Omega_t)}{v_t} && (12) \\ \beta_{ri} &= \delta_2 - \tan^{-1}\frac{(w_i - e\Omega_i)}{v_i} && (13) \end{aligned}$$

The lateral forces $\{F_{lf}, F_{lr}, F_{li}\}^T$ can then be calculated using,

$$\begin{aligned} F_{lf} &= k_s \beta_{tf} && (14) \\ F_{lr} &= k_s \beta_{tr} && (15) \\ F_{li} &= k_s \beta_{ri} && (16) \end{aligned}$$

where k_s is a constant.

B. Non-slip Model

In the non-slip model, the β's in equations (11)-(13) must be zero. Hence we obtain, three new conditions,

$$\tan\delta_1 = -\frac{(w_t + a\Omega_t)}{v_t} \quad (17)$$
$$w_t = b\Omega_t \quad (18)$$
$$\tan\delta_2 = \frac{(w_i - e\Omega_i)}{v_i} \quad (19)$$

Equations (1),(2) and (17)-(19) can be solved to obtain a matrix S such that,

$$\begin{bmatrix} v_i & w_i & \Omega_t & \Omega_i \end{bmatrix}^T = S\ v_i \quad (20)$$

By differentiating,

$$\begin{bmatrix} \dot{v}_i & \dot{w}_i & \dot{\Omega}_t & \dot{\Omega}_i \end{bmatrix}^T = S\ \dot{v}_i + \dot{S}\ v_i \quad (21)$$

Substituting in (4),

$$DS\dot{v}_i + D\dot{S}v_i + G_{1_1}\begin{bmatrix} F_{lf} \\ F_{lr} \\ F_{li} \end{bmatrix} + G_2\begin{bmatrix} T_{tf} \\ T_{tr} \end{bmatrix} + G_0 = 0 \quad (22)$$

Equation (22) represents four equations in $\{\dot{v}_i, F_{lf}, F_{lr}, F_{li}\}$. They can be used to solve for $\dot{v}_i$. The solution can also be obtained by pre-multiplying (22) by S^T. This gives,

$$S^T DS\dot{v}_i + S^T D\dot{S}v_i + S^T G_{1_1}\begin{bmatrix} F_{lf} \\ F_{lr} \\ F_{li} \end{bmatrix} + S^T G_2\begin{bmatrix} T_{tf} \\ T_{tr} \end{bmatrix} + S^T G_0 = 0 \quad (23)$$

It can be shown that $S^T G_{1_1} = 0$. Hence, the non-slip dynamic model is,

$$\dot{v}_i = -(S^T DS)^{-1}\left(S^T D\dot{S}v_i + S^T G_2\begin{bmatrix} T_{tf} \\ T_{tr} \end{bmatrix} + S^T G_0\right) \quad (24)$$

Equations (24), (5)-(7) form the complete set of dynamic equations for the non-slip model with the state vector of $\{v_i, \phi, \delta_1, \delta_2\}^T$ and a control input vector of $\{T_{tf}, T_{tr}, F_{st}, F_{si}\}^T$.

III. MODEL SIMULATION

With the model obtained in Section II, the tractor-implement system is simulated under varying conditions. The parameters and constants of the model have only been partially verified, with known parameters based on an existing John Deere compact agricultural tractor. All remaining and unknown parameters are believed to be realistic for the tractor and conditions at hand.

Four simulations of the tractor-implement system are presented, and show the trajectories of the tractor and/or implement centre of mass. The results which are outlined following, firstly compare the response of the tractor-implement system under no-slip and slip conditions. In the no-slip case, the tractor and implement wheels are constrained to their intended paths going around bends, not unlike a train which is constrained to its track. The second comparison is made under slip conditions, by applying two different magnitude disturbance forces to both the tractor and implement. Such disturbances are restricted to point in one direction, and are meant to mimic the effects of operating the tractor and implement on sloping ground with differing grades.

In each following simulation, the tractor and implement are assumed to start at rest, are in alignment with each other, and have orientations of zero degrees. On the simulation plots, this corresponds to the combination pointing from left to right. In each case, the traction, or propulsion forces are set to constants, with $T_{ft} = 500$, and $T_{rt} = 2000$. After 15 seconds of motion with the steered wheels pointing directly ahead, the front wheels of the tractor are actuated resulting in a wheel displacement of approximately 25^o (turn to the right) for 1.5 seconds. At this point the front tractor wheels are actuated in the reverse direction (left) such that they are once again pointing straight ahead.

The disturbance forces F_t and F_i are applied to the tractor and implement in the negative y direction, corresponding from top to bottom on the following simulation plots. In the dynamic model, the direction of these disturbance forces is specified with respect to the axes of the tractor and implement. As the orientation of both the tractor and implement changes, these force angles are transformed to give a fixed direction.

The four simulations may be briefly described as follows:

Case 1: Without slip, without lateral disturbances.

Here, the slip angles, β_{tf}, β_{tr}, and β_{ri} are identically zero, and the lateral slip forces have no effect on the model. The no-slip model derived above is implemented. Fig. 2 shows the animated trajectory of the tractor and implement as it is going into, and coming out of, the right hand turn.

Case 2: With slip, without lateral disturbances.

Fig. 3 displays the trajectory of the tractor and implement for this case. As with the no-slip case, the plot focuses on the curved part of the trajectory resulting from actuating the steering. The slip model of Section II is used with the disturbance forces F_t and F_i set to zero.

Case 3: With slip, with small lateral disturbances.

As with Case 2, however each lateral disturbance force is set such that its effect is equivalent to that obtained by operating on a sloping ground. The slope is downward in the negative y direction (top to bottom on the plot) with a grade of approximately 2%. From the perspective of the tractor, it effectively starts its operation driving across the slope and then turns right down the slope.

Case 4: With slip, with large lateral disturbances.

Similar to Case 3, with larger lateral disturbance forces. Their effect is to simulate a ground slope with a grade of approximately 10% in the same direction.

The plots of Fig. 4 depict the complete trajectories of the tractor alone for each of the four cases.

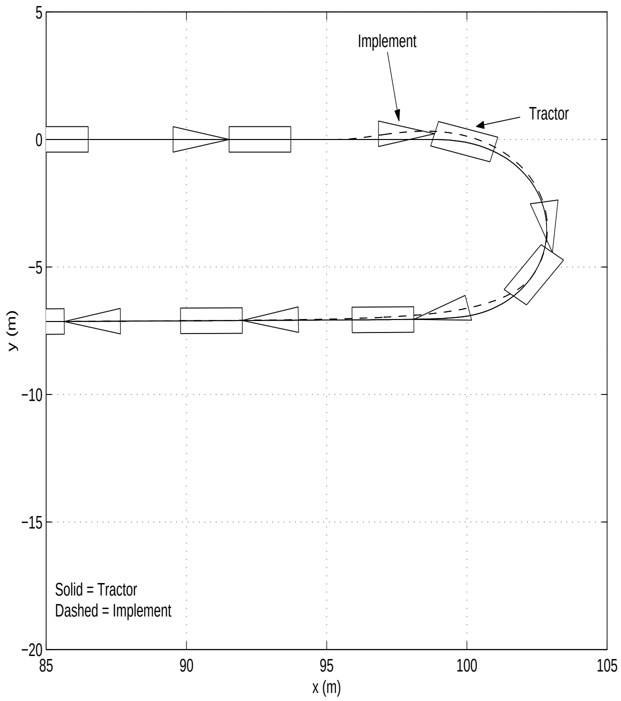

Fig. 2. Tractor-Implement trajectory under no-slip condition

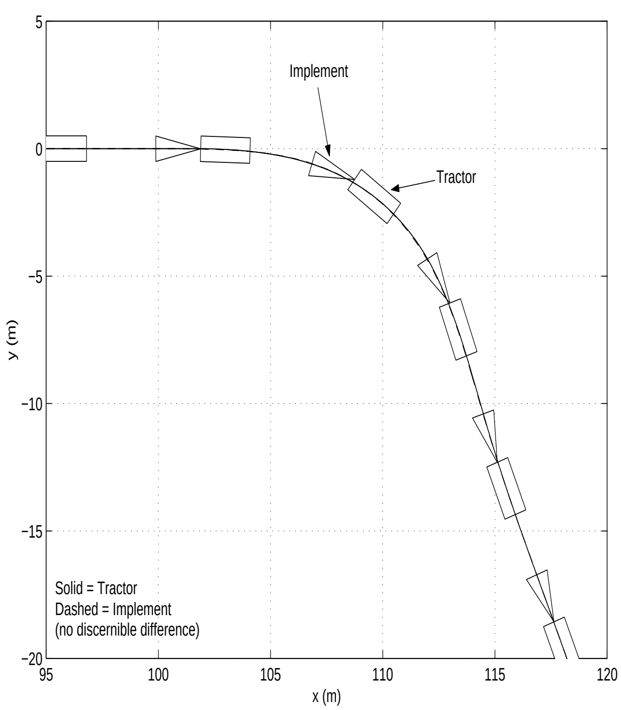

Fig. 3. Tractor-Implement trajectory with slip, no disturbances

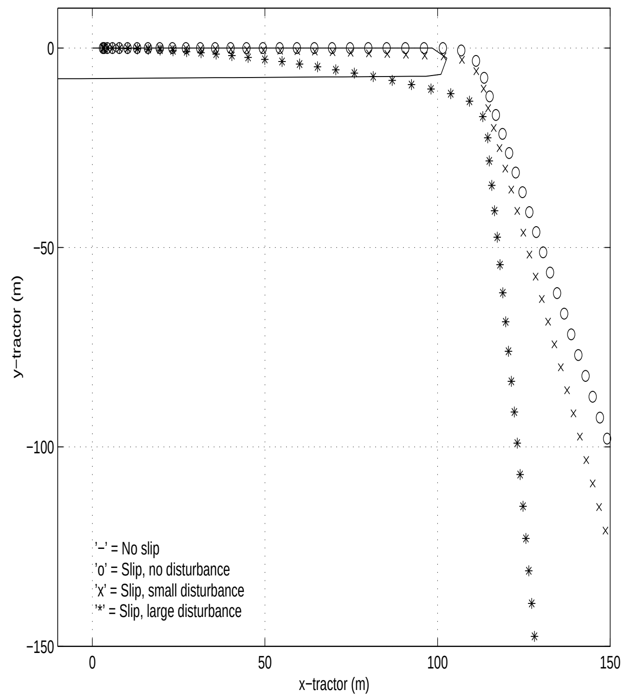

Fig. 4. Tractor trajectories for all cases

IV. DISCUSSION

The results shown in Fig. 2, Fig. 3, and Fig. 4, show some significant and telling differences between the different simulations. Although these results are not experimentally verified as yet, they give a quite good account of how the tractor-implement pair would behave.

When comparing the no-slip and slip simulations, the trajectories start to diverge as soon as steering actuation is applied, as would be expected. Differences exist not only in the final steady-state heading of the tractor and implement, but also in the curved motion under non-zero steering angle. In Fig. 2 and Fig. 3, it is seen that the radius of curvature for the no-slip case is somewhat smaller. In addition, differences can be seen between the no-slip tractor and implement responses. Once steering is commenced, the implement receives a small "kick" outwards due to the outward reaction of the rear hitch-point of the tractor. However the implement soon recovers and finishes the curve with its centre of mass trajectory inside that of the tractor. This characterisitic would be expected of a chained system with constrained (no slip) motion. On the other hand, when the slip model is applied, it can be seen that the implement center of mass trajectory remains close to that of the tractor, indicating that the rear of the implement is sliding outward. Once the steering actuation has concluded however, and the tractor aligns to a straight path, the implement also self-aligns to the tractor again.

The lateral slip forces in (14)-(16) suggest a linear relationship between the slip angles and the resulting forces. In [21], this linear relationship is similarly used. In reality though, the lateral slip forces tend to saturate above a certain threshold, which for simulation purposes was taken to be in the range $5^o - 10^o$ for this tractor and implement. It was noted that the inclusion of this saturation in the simulation had the effect of reducing the slipping of both tractor and implement. An additional variation between this work and that of [21] is the value of the slip angle gain k_s. A smaller gain is applied here to take into account the extra uncertainty in ground conditions in an agriculural setting. It was also noted that uncertainty in the slip angle gain lead to quite marked changes in the amount of exhibited slip and thus the trajectories of the tractor and implement. This fact suggests more comprehensive and experimental modeling of the type slip will be required.

From Fig. 4, the effect of applying lateral disturbance forces is seen. It is important to keep in mind that the simulations undertaken are completely in open-loop, and no effort is made to correct either the tractor's or implement's trajectory in the event that such forces cause them to stray from their intended paths. As expected, the larger lateral force gives rise to more tractor and implement drift on the first straight. More specifically, both tractor and implement drift approximately 10m "down" the slope for 100m of forward motion, as opposed to a 2m drift for the smaller lateral force. Also, at the conclusion of the turn, when the tractor and implement are generally pointing in the direction of the force (down the slope), the larger force results in a greater speed and hence greater distance travelled.

An important feature of this simulation is the inclusion of not only the tyre rolling resistance forces, but also an implement dragging force. The dragging force would be present on an implement with seeding tines for example, and cannot be ignored. Without the presence of the rolling resistance force, the tractor and implement would continue to accelerate unrealistically.

V. CONCLUSIONS

This paper presents a comprehensive and realistic dynamic model of a tractor-implement combination. A feature of the model is that it is subject to real conditions and real disturbances more applicable in an agricultural setting such as broad acre cropping. Such real conditions include ground uncertainty, sloping terrain, type slip, and the existence of rolling, or drag, forces, which act against the forward motion of the tractor.

Highlighted was the derivation of both a slip, and no-slip model for the purpose of comparison. Application of the models showed the significant effect that slip has on the trajectory of both the tractor and implement. The importance of this phenomenom cannot be understated as it can be a significant problem in a precision farming setting. On an implement with seeding tines at its rear, for example, such sliding motion can result in the tines being applied with significant error.

In addition, the application of lateral disturbance forces underlines the requirement that a controller be sufficiently robust in order to maintain both implement and tractor on their desired paths. Once again, such lateral forces are particularly relevant in an agricultural or precision farming environment, where ground undulation and sloping terrain may play a role.

Importantly, the models, and the results from the models, provide a sound basis for which to continue research into precision implement guidance. It will be necessary to carry out experimental model validation to confirm these results. This will be undertaken with an existing John Deere compact agricultural tractor and an appropriate implement to be designed and constructed.

In parallel, work can now be undertaken in designing and testing different advanced, and mostly nonlinear, controllers. With significant precision required for implement guidance, and with the demonstrated effects of tyre slip and disturbance forces, this will be a challenging and non-trivial task.

APPENDIX

$$D = \begin{bmatrix} m_i + m_t & 0 & (b+c)m_t \sin\phi & 0 \\ 0 & m_i + m_t & (b+c)m_t\cos\phi & d\ m_t \\ (b+c)m_t\sin\phi & (b+c)m_t\cos\phi & J_t + (b+c)^2 m_t & (b+c)d\ m_t\cos\phi \\ 0 & d\ m_t & (b+c)d\ m_t\cos\phi & J_i + d^2 m_t \end{bmatrix} \tag{25}$$

$$G_{1_1} = \begin{bmatrix} \sin(\phi+\delta_1) & \sin\phi & -\sin\delta_2 \\ \cos(\phi+\delta_1) & \cos\phi & \cos\delta_2 \\ (a+b+c)\cos\delta_1 & c & 0 \\ d\cos(\phi+\delta_1) & d\cos\phi & -e\cos\delta_2 \end{bmatrix} \tag{26}$$

$$G_{1_2} = \begin{bmatrix} \cos(\phi+\delta_1) & \cos\phi & \cos\delta_2 & \cos(\beta_{ri}-\delta_2) \\ -\sin(\phi+\delta_1) & -\sin\phi & \sin\delta_2 & -\sin(\beta_{ri}-\delta_2) \\ -(a+b+c)\sin\delta_1 & 0 & 0 & 0 \\ -d\sin(\phi+\delta_1) & -d\sin\phi & -e\sin\delta_2 & e\sin(\beta_{ri}-\delta_2) \end{bmatrix} \tag{27}$$

$$G_2 = \begin{bmatrix} -\cos(\phi+\delta_1) & -\cos\phi & -\cos\delta_2 \\ \sin(\phi+\delta_1) & \sin\phi & -\sin\delta_2 \\ (a+b+c)\sin\delta_1 & 0 & 0 \\ d\sin(\phi+\delta_1) & d\sin\phi & e\sin\delta_2 \end{bmatrix} \tag{28}$$

$$G_3 = \begin{bmatrix} -\cos\alpha_i & -\cos(\phi+\alpha_t) \\ \sin\alpha_i & \sin(\phi+\alpha_t) \\ 0 & (b+c)\sin\alpha_t \\ 0 & d\sin(\phi+\alpha_t) \end{bmatrix} \tag{29}$$

$$G_0 = \begin{bmatrix} -(m_i+m_t)w_i\Omega_i - dm_t\Omega_i^2 - (b+c)m_t\cos\phi\Omega_t^2 \\ (m_i+m_t)v_i\Omega_i + (b+c)m_t\sin\phi\Omega_t^2 \\ (b+c)m_t\Omega_i(v_i\cos\phi - w_i\sin\phi - d\Omega_i\sin\phi) \\ dm_t v_i\Omega_i + d(b+c)m_t\sin\phi\Omega_t^2 \end{bmatrix} \tag{30}$$

The matrix $S^T = \{s_1, s_2, s_3, s_4\}$ is such that,

$$\begin{aligned} s_1 &= 1 \\ s_2 &= \frac{c(\cos\phi\tan\delta_1 - (a+b)\sin\phi)/s_0 + d\tan\delta_2}{d+e} \\ s_3 &= \frac{\tan\delta_1}{s_0} \\ s_4 &= \frac{(\cos\phi\tan\delta_1 - (a+b)\sin\phi)/s_0 + \tan\delta_2}{d+e} \end{aligned}$$

where

$$s_0 = (a+b)\cos\phi + c\sin\phi\tan\delta_1$$

Note that $S^T G_{1_1} = 0$. Hence the third term of (23) will disappear.

REFERENCES

[1] Richard M. Murray, Zexiang Li, and S. Shankar Sastry. *A Mathematical Introduction to Robotic Manipulation*. CRC Press, Boca Raton, 1994.

[2] Rajesh Rajamani. *Vehicle Dynamics and Control*. Springer, New York, 2006.

[3] Claudio Altafini, Alberto Speranzon, and Bo Wahlberg. A feedback control scheme for reversing a truck and trailer vehicle. *IEEE Tran. on Robotics and Automation*, 17(6):915–922, December 2001.

[4] P. J. Smith, D. R. Lindgren, T. Hague, and J. A. Marchant. Relating torque and slip in an odometric model for an autonomous agricultural vehicle. *Autonomous Robot*, 13(1):73–86, July 2002.

[5] M. Lida, M. Kudou, K. Ono, and M. Umeda. Automatic following control for agricultural vehicle. In *In Proceedings of the 6th International Workshop on Advanced Motion Control*, pages 158–162, Nagoya, Japan, 2000.

[6] R. Lenain, B. Thuilot, C. Cariou, and P. Martinet. Adaptive control of car like vehicles guidance relying on RTK-GPS: Rejection of sliding effects in agricultural applications. In *Proceedings of IEEE International Conference of Robotics and Automation*, pages 115–120, Taipei, Taiwan, September 2003.

[7] Q. Zhang and H. Qiu. A dynamic path search algorithm for tractor automatic navigation. *Transactions of the American Society of Agricultural Engineers*, 47(2):639–646, March/April 2004.

[8] M. F. Kocher, M. B. Smith, R. D. Grisso, and L. L. Bashford. Performance tests of three point mounted implement guidance systems, I. *Journal of Applied Engineering in Agriculture*, 16(6):595–603, November 2000.

[9] M.F. Kocher, M.B. Smith, R.D. Grisso, and L. J. Young. Performance tests of three point mounted implement guidance systems, II. *Journal of Applied Engineering in Agriculture*, 16(6):605–611, November 2000.

[10] J. Katupitiya, R. Eaton, G. Rodnay, A. Cole, and C. Meyer. Automation of an agricultural tractor for fruit picking. In *IEEE International Conference on Robotics and Automation*, page (to appear), Barcelona, Spain, April 2005.

[11] R. Eaton, J. Katupitiya, A. Cole, and C. Meyer. Architecture of an automated agricultural tractor: Hardware, software and control systems. In *In Proceedings of the 16th World Congress of the IFAC*, page (to appear), Prague, Czech Republic, July 2005.

[12] Andrew J. Scarlett. Integrated control of agricultural tractors and implements: a review of potential opportunities relating to cultivation and crop establishment machinery. *Computer and Electronics in Agriculture*, 30:167–191, 2001.

[13] H. Fang, R. Fan, B. Thuilot, and P. Martinet. Trajectory tracking control of farm vehicles in presence of sliding. *Robotics and Autonomous Systems*, 54:828–839, 2006.

[14] Lei Feng, Yong He, Yidan Bao, and Hui Fang. Development of trajectory model for a tractor-implement system for automated navigation applications. *Proceedings of the IEEE Instrumentation and Measurement Technology Conference (IEEE Cat. No.05CH37627C)*, pages 5 pp. –, 2005.

[15] M.G. Yisa, H. Terao, N. Noguchi, and M. Kubota. Stability criteria for tractor-implement operation on slopes. *Journal of Terramechanics*, 35, 1998.

[16] R. Lenain, B. Thuilot, C. Cariou, and P. Martinet. High accuracy path tracking for vehicles in presence of sliding: application to farm vehicle automatic guidance for agricultural tasks. *Auton. Robots (Netherlands)*, 21(1):79–97, August 2006.

[17] R. Lenain, B. Thuilot, C. Cariou, and P. Martinet. Sideslip angles observer for vehicle guidance in sliding conditions: Application to agricultural path tracking tasks. In *Proceedings of the 2006 IEEE International Conference on Robotics and Automation*, pages 3183–3188, Orlando, FL, USA, May 2006.

[18] D.W.M. Pullen and P.A. Cowell. Prediction and experimental verification of the hoe path of a rear-mounted inter-row weeder. *Journal of Agricultural Engineering Research*, 77(2):137–153, October 2000.

[19] D.W.M. Pullen and P.A. Cowell. The effect of implement geometry on the hoe path of a steered rear-mounted inter-row weeder. *Biosystems Engineering*, 94(3):373–386, July 2006.

[20] Lei Feng, Yong He, and Qin Zhang. Tractor-implement dynamic trajectory model for automated navigation applications. *Proceedings - 3rd International Conference on Information Technology and Applications, ICITA 2005*, I:330–335, 2005.

[21] R. M. DeSantis. Path-tracking for a tractor-trailer like robot. *The International Journal of Robotics Research*, 13(6):533–544, December 1994.